JOC Article

Toward an Understanding of the Unexpected Regioselective Hetero-Diels−Alder Reactions of Asymmetric Tetrazines with Electron-Rich Ethylenes: A DFT Study†

Luis R. Domingo,* M. Teresa Picher, and José A. Sáez

Departamento de Química Orgánica, Universidad de Valencia, Dr. Moliner 50, 46100 Burjassot, Valencia, Spain

domingo@utopia.uv.es

Received December 30, 2008

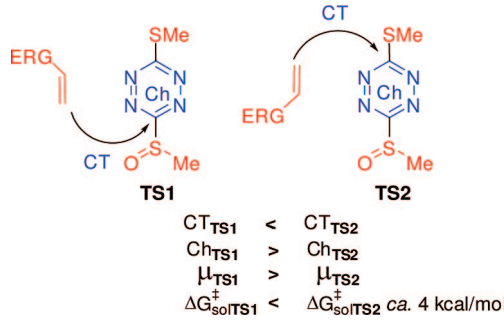

The regioselective hetero-Diels−Alder (HDA) reaction of asymmetric tetrazines (TTZs) with electron-rich (ER) ethylenes has been studied with use of DFT methods at the B3LYP/6-31G* level of theory. The reaction is a domino process that comprises three consecutive reactions: (i) a HDA reaction between the TTZ and the ER ethylene; (ii) a retro-Diels−Alder reaction with loss of nitrogen; and (iii) a β-hydrogen elimination with formation of the final pyridazines. The first polar HDA reaction, which is associated to the nucleophilic attack of the ER ethylene to the electrophilically activated TTZ, is the rate and regioselectivity determining step of the domino process. The unexpected regioselectivity of these HDA reactions is explained within the polar cycloaddition model by using the conceptual DFT. Although the nucleophilic attack of the ER ethylene over the *para* position relative to the methylsulfinyl substituent could favor the charge transfer, it is energetically more unfavorable because it diminishes the electron density at the electronegative TTZ core.

Introduction

1,2,4,5-Tetrazine (**1**) has proven to be an useful reagent that participates in hetero-Diels−Alder (HDA) reactions with a wide range of dienophiles and heterodienophiles, providing rapid access to a range of highly substituted pyridazines and related heterocycles.[1] The expected bicyclic intermediates, **BcIN1** and **BcIN2**, have never been observed; the reaction product is that obtained by loss of nitrogen (see Scheme 1). When the dienophile is an alkyne, the loss of nitrogen forms an aromatic ring directly.

SCHEME 1

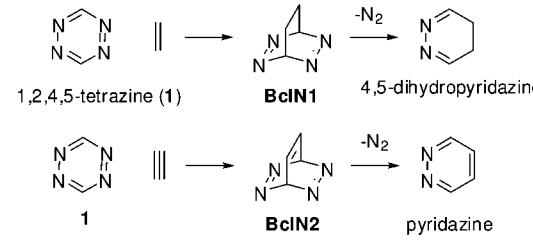

Typically, symmetrical tetrazines (TTZs) are employed largely due to their synthetic accessibility. Trends in reactivity of TTZs have been explored in some detail by Boger and co-

† Dedicated to Prof. S. Olivella on occasion of his 65th birthday.

(1) (a) Boger, D. L.; Weinreb, S. M. *Hetero Diels-Alder Methodology in Organic Synthesis*; Academic Press: San Diego, CA, 1987. (b) Sauer, J. *Comprehensive Heterocyclic Chemistry II*; Pergamon: London, UK, 1996; Vol. 6, pp 901−965. (c) Boger, D. L.; Coleman, R. S.; Panek, J. P.; Huber, F. X.; Sauer, J. *J. Org. Chem.* **1985**, *50*, 5377–5379. (d) Warrener, R. N.; Margetic, D.; Amarasekara, A. S.; Butler, D. N.; Mahadevan, I. B.; Russell, R. A. *Org. Lett.* **1999**, *1*, 199–202. (e) Yeung, B. K. S.; Boger, D. L. *J. Org. Chem.* **2003**, *68*, 5249–5253.

10.1021/jo802822u CCC: $40.75
Published on Web 03/04/2009

CHART 1

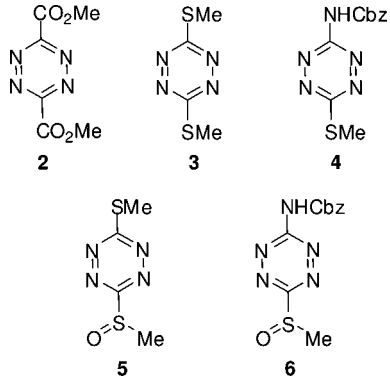

SCHEME 2

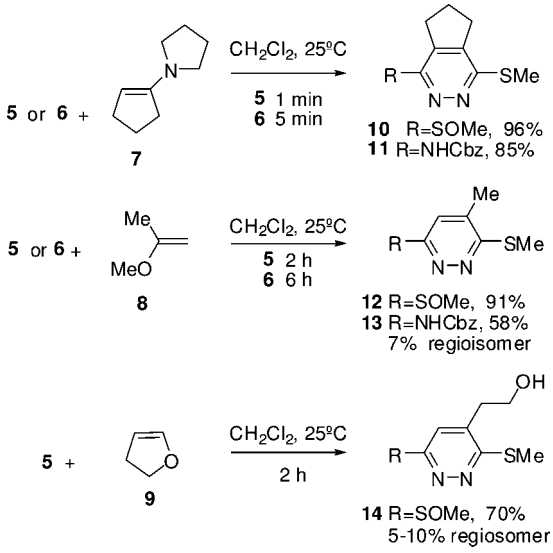

workers,[2] introducing several symmetrical, such as dimethyl 3,6-dicarboxylate[3] (**2**) and 3,6-*bis*(thiomethyl)-1,2,4,5-tetrazine[4] (**3**), and asymmetrical TTZs, such as *N*-acyl-3-amino-6-methylthio-1,2,4,5-tetrazine[5] (**4**) (see Chart 1).

Recently, Boger et al. have reported the HDA reactions of two new asymmetrically substituted TTZs, 3-methylsulfinyl-6-thiomethyl-1,2,4,5-tetrazine (**5**) and 3-(benzyloxycarbonyl)amino-6-methylsulfinyl-1,2,4,5-tetrazine (**6**), obtained by sulfur oxidation of **3** and **4**, toward a series of electron-rich (ER) ethylenes.[6] These new TTZs displayed greater reactivity than **3** or **4**, due to their enhanced electron-deficient (ED) character. The products of the HDA reactions of the TTZs **5** and **6** were the pyridazines **10**–**14** obtained by HX (X = OR or NR_2) elimination (see Scheme 2). The HDA reactions of **5** and **6** were regioselective, producing typically a single pyridazine, as can be seen in the reaction of **5** with **8**, which gives the product **12**. However, the observed regioselectivity was opposite to that anticipated on the basis of simple zwitterionic models derived from a frontier molecular orbital (FMO) analysis. Boger indicated that only the LUMO energy level of the FMO analysis

SCHEME 3

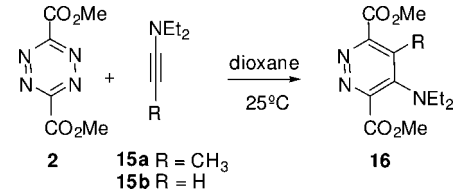

SCHEME 4

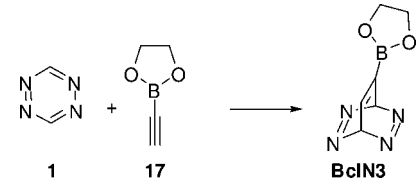

reflects accurately the reactivity increase of **5** and **6** relative to **3** and **4**.[6] Further treatment of TTZ **5** with Et_2NH as nucleophile only provided the product derived from the displacement of the methylsulfinyl group and not the methyl sulfide.[6] Consequently, Boger et al. suggested that the reaction could proceed through stepwise addition–cyclization reactions initialized by a nucleophilic addition.

The HDA reactions of some simple TTZs with acetylene derivatives to yield pyridazines have been theoretically studied. Sauer et al. performed an earlier experimental and ab initio (HF/6-31G** and MP2/6-31G**) study about the HDA reaction of TTZ **1** with acetylene and phenylacetylene.[7] Ab initio calculations about the HDA reaction of **1** with acetylene indicated that this reaction takes place through a synchronous concerted transition state structure (TS), with a distance between the interacting pair of atoms of 2.161 Å (MP2 results). While HF overestimated the activation energy, 42.1 kcal/mol, MP2 calculations underestimated it, 11.5 kcal/mol. The loss of nitrogen had a low barrier, 5.5 kcal/mol (HF), making the reaction very exothermic, −93.1 kcal/mol (HF).

Recently, Birney et al. reported an experimental and theoretical study about the sequential TSs involved in the HDA reactions of symmetrically substituted TTZ **2** with the ER alkyne **15a** (see Scheme 3).[8] Kinetic measurements of the HDA reactions of **2** with **15a** gave a $\Delta G^{\#}$ of 11.5 kcal/mol, a value that was 7.7 kcal/mol lower in energy than that for the reaction of **2** with acetylene. Calculations at B3LYP/6-31G** level for the HDA reaction of TTZ **2** with **15b** showed that it takes place through a concerted but very asynchronous TS; the forming bond distances were 1.892 and 2.944 Å. The computed barrier of the HDA reaction was 7.6 kcal/mol. The intermediate **BcIN2**-type, formed with a very low barrier, 1.5 kcal/mol, loses nitrogen via one synchronous TS to yield the pyridazine **16**.

Very recently, Gomez-Bengoa et al. studied the participation of alkynylboronates in DA reactions.[9] B3LYP/6-31G* calculations were performed to study the HDA reaction of the simplest TTZ **1** with alkynylboronate **17** to yield the bicyclic intermediate **BcIN3** (see Scheme 4). This HDA reaction has a concerted mechanism via a synchronous TS (forming bond distances of 2.17 and 2.23 Å) and proceeds with a large activation barrier,

(2) Soenen, D. R.; Zimpleman, J. M.; Boger, D. L. *J. Org. Chem.* **2003**, *68*, 3593–3598.
(3) Boger, D. L.; Hong, J. *J. Am. Chem. Soc.* **2001**, *123*, 8515–8519.
(4) Boger, D. L.; Sakya, S. M. *J. Org. Chem.* **1988**, *53*, 1415–1423.
(5) Boger, D. L.; Schaum, R. P.; Garbaccio, R. M. *J. Org. Chem.* **1998**, *63*, 6329–6337.
(6) Hamasaki, A.; Ducray, R.; Boger, D. L. *J. Org. Chem.* **2006**, *71*, 185–193.
(7) Cioslowski, J.; Sauer, J.; Hetzenegger, J.; Karcher, T.; Hierstetter, T. *J. Am. Chem. Soc.* **1993**, *115*, 1353–1359.
(8) Sadasivam, D. V.; Prasad, E.; Flowers, R. A.; Birney, D. M. *J. Phys. Chem. A* **2006**, *110*, 1288–1294.
(9) Gomez-Bengoa, E.; Helm, M. D.; Plant, A.; Harrity, J. P. A. *J. Am. Chem. Soc.* **2007**, *129*, 2691–2699.

20.4 kcal/mol. This large value agreed with the high temperature required by the experimental reaction, 140 °C. Analysis of the charge transfer (CT) at the TS indicated that it takes place from the alkynylboronate **17** to TTZ **1**. This fact was confirmed by the large electrophilicity of TTZ **1**, 3.38 eV, compared with that of the alkynylboronate **17**, 0.83 eV. In spite of the large electrophilic character of TTZ **1**, the symmetry of the simplest TTZ **1** appears to be responsible for the large activation barrier and the concerted character of this HDA reaction.[9,10]

While the HDA reaction of TTZs with acetylenes has been studied, the HDA reaction with ethylenes has not been theoretically treated. The large electrophilic character of the TTZ **1**, together with the low barrier computed for the HDA reaction of the disubstituted TTZ **2** with the ER acetylene **15b** point out the large polar character of these HDA reactions. Our interest for the mechanisms of polar Diels−Alder reactions instigated us to carry out a theoretical study of the mechanism of the regioselective HDA reactions of the electrophilically activated asymmetric TTZs studied by Boger.[6] The unexpected regioselectivity showed by the HDA reactions of the asymmetrically substituted TTZ **5** makes these reactions an appropriate model for a density functional theory (DFT) study. First, an analysis of the reactivity indexes defined within the conceptual DFT will be used to explain the polar character of these HDA reactions. Then, the domino reaction of the TTZ **5** toward the vinylamine **7** to yield the pyridazine **10**, which represents the faster HDA reaction of those studied by Boger,[6] will be analyzed. Finally, the HDA reaction of the TTZ **5** toward the vinyl ethers **8** and **9** will be performed to explain the regioselectivity experimentally observed by Boger. The polar character of the HDA reactions of these asymmetric TTZs as well as the regioselectivity experimentally observed will be analyzed.

Computational Methods

DFT calculations were carried out with use of the B3LYP[11] exchange-correlation functionals, together with the standard 6-31G* basis set. Since some species involved in these HDA reactions have some zwitterionic character, the effects of the diffuse functions on the geometries and energies on the HDA reaction between the TTZ **5** and the vinyl amine **7** were analyzed by using the 6-31+G** basis set.[12] The inclusion of diffuse functions on the geometry optimization does not produce significant geometry or energy changes (see later). The optimizations were carried out with the Berny analytical gradient optimization method.[13] The stationary points were characterized by frequency calculations to verify that TSs had one and only one imaginary frequency. The intrinsic reaction coordinate (IRC)[14] path was traced to check the energy profiles connecting each TS to the two associated minima of the proposed mechanism, using the second-order González−Schlegel integration method.[15] The values of enthalpies, entropies, and free energies were calculated with the standard statistical thermodynamics at 298.15 K.[12] Thermodynamic calculations were scaled by an empirical factor of 0.96.[16] The electronic structures of stationary points were analyzed by the NBO method.[17] All calculations were carried out with the Gaussian 03 suite of programs.[18]

Solvent effects have been considered at the same level of theory by single-point energy calculations over the gas-phase structures, using a self-consistent reaction field (SCRF)[19] based on the polarizable continuum model (PCM) of Tomasi's group.[20] Since these cycloadditions are carried out in dichloromethane, we have selected its dielectric constant at 298.0 K, $\varepsilon = 8.93$, and a solvent radius of 2.27 Å. The cavity is created via a series of overlapping spheres centered on the atoms, using the simple united atom topological (UA0) model, i.e., by putting a sphere around each solute heavy atom; hydrogen atoms are enclosed in the sphere of the atom to which they are bonded.

The global electrophilicity index,[21] ω, which measures the energy stabilization when the system acquires an additional electronic charge ΔN from the environment, has been given by the following simple expression,[21] $\omega = (\mu^2/2\eta)$, in terms of the electronic chemical potential μ and the chemical hardness η. Both quantities may be approached in terms of the one-electron energies of the frontier molecular orbital HOMO and LUMO, ε_H and ε_L, as $\mu \approx (\varepsilon_H + \varepsilon_L)/2$ and $\eta \approx (\varepsilon_L - \varepsilon_H)$, respectively.[22] Recently, we have introduced an empirical (relative) nucleophilicity index,[23] N, based on the HOMO energies obtained within the Kohn−Sham scheme,[24] and defined as $N = E_{HOMO(Nu)} - E_{HOMO(TCE)}$. This nucleophilicity scale is referred to tetracyanoethylene (TCE) taken as a reference. The reactivity indexes were computed from the B3LYP/6-31G* HOMO and LUMO energies at the ground state of the molecules.

Results and Discussions

Analysis Based on the Reactivity Indexes at the Ground State of Reagents. Recent studies devoted to DA reactions have shown that the global indexes defined within the context of density functional theory[25] are a powerful tool to understand the behavior of polar cycloadditions.[26] In Table 1, we report the static global properties, namely, electronic chemical potential μ, chemical hardness η, global electrophilicity ω, and nucleophilicity N, of the TTZs **1**, **2**, **5**, and **6** and the ER ethylenes **7** and **8**.

The electronic chemical potential of the TTZs, $\mu = -0.1707$ to -0.1883 au, is lower than the electronic chemical potential of ER ethylenes **7**, **8**, and **9**, $\mu = -0.0852$ to -0.0534 au, respectively, indicating thereby that along these HDA reactions,

(10) Domingo, L. R.; Aurell, M. J.; Perez, P.; Contreras, R. *J. Org. Chem.* **2003**, *68*, 3884–3890.
(11) (a) Becke, A. D. *J. Chem. Phys.* **1993**, *98*, 5648–5652. (b) Lee, C.; Yang, W.; Parr, R. G. *Phys. Rev. B* **1988**, *37*, 785–789.
(12) Hehre, W. J.; Radom, L.; Schleyer, P. v. R.; Pople, J. A. *Ab initio Molecular Orbital Theory*; Wiley: New York, 1986.
(13) (a) Schlegel, H. B. Geometry Optimization on Potential Energy Surface. In *Modern Electronic Structure Theory*; Yarkony, D. R., Ed.; World Scientific Publishing: Singapore, 1994. (b) Schlegel, H. B. *J. Comput. Chem.* **1982**, *3*, 214–218.
(14) Fukui, K. *J. Phys. Chem.* **1970**, *74*, 4161–4163.
(15) (a) Gonzalez, J.; Houk, K. N. *J. Org. Chem.* **1992**, *57*, 3031–3037. (b) Gonzalez, J.; Taylor, E. C.; Houk, K. N. *J. Org. Chem.* **1992**, *57*, 3753–3755.
(16) Scott, A. P.; Radom, L. *J. Phys. Chem.* **1996**, *100*, 16502–16513.
(17) (a) Reed, A. E.; Curtiss, L. A.; Weinhold, F. *Chem. Rev.* **1988**, *88*, 899–926. (b) Reed, A. E.; Weinstock, R. B.; Weinhold, F. *J. Chem. Phys.* **1985**, *83*, 735–746.
(18) Frisch, M. J.; et al. *Gaussian 03*, Revision C.02; Gaussian, Inc., Wallingford, CT, 2004.
(19) (a) Tomasi, J.; Persico, M. *Chem. Rev.* **1994**, *94*, 2027–2094. (b) Simkin, B. Y.; Sheikhet, I. *Quantum Chemical and Statistical Theory of Solutions−A Computational Approach*; Ellis Horwood: London, UK, 1995.
(20) (a) Cances, E.; Mennucci, B.; Tomasi, J. *J. Chem. Phys.* **1997**, *107*, 3032–3041. (b) Cossi, M.; Barone, V.; Cammi, R.; Tomasi, J. *Chem. Phys. Lett.* **1996**, *255*, 327–335. (c) Barone, V.; Cossi, M.; Tomasi, J. *J. Comput. Chem.* **1998**, *19*, 404–417.
(21) Parr, R. G.; von Szentpaly, L.; Liu, S. *J. Am. Chem. Soc.* **1999**, *121*, 1922–1924.
(22) (a) Parr, R. G.; Pearson, R. G. *J. Am. Chem. Soc.* **1983**, *105*, 7512–7516. (b) Parr, R. G.; Yang, W. *Density Functional Theory of Atoms and Molecules*; Oxford University Press: New York, 1989.
(23) Domingo, L. R.; Chamorro, E.; Pérez, P. *J. Org. Chem.* **2008**, *73*, 4615–4624.
(24) Kohn, W.; Sham, L. J. *Phys. Rev.* **1965**, *140*, 1133–1138.
(25) (a) Geerlings, P.; De Proft, F.; Langenaeker, W. *Chem. Rev.* **2003**, *103*, 1793–1873. (b) Ess, D. H.; Jones, G. O.; Houk, K. N. *Adv. Synth. Catal.* **2006**, *348*, 2337–2361.
(26) (a) Domingo, L. R.; Aurell, M. J.; Perez, P.; Contreras, R. *Tetrahedron* **2002**, *58*, 4417–4423. (b) Pérez, P.; Domingo, L. R.; Aizman, A.; Contreras, R. In *Theoretical Aspects of Chemical Reactivity*; Toro-Labbé, A., Ed.; Elsevier Science: Amsterdam, The Netherlands, 2007; Vol. 19, pp 139−201.

TABLE 1. Electronic Chemical Potential (μ, in au), Chemical Hardness (η, in au), Global Electrophilicity (ω, in eV) and Global Nucleophilicity (N, in eV) of the Tetrazines 1−3, 5, and 6 and the ER Ethylenes 7, 8, and 9

	μ	η	ω	N
5	−0.1819	0.1209	3.72	2.52
6	−0.1818	0.1216	3.70	2.52
2	−0.1883	0.1324	3.64	2.20
1	−0.1832	0.1349	3.38	2.30
3	−0.1707	0.1280	3.10	2.48
9	−0.0852	0.2668	0.37	3.17
8	−0.0808	0.2468	0.36	3.56
7	−0.0534	0.2290	0.17	4.55

the net CT will take place from the ER ethylenes toward these ED TTZs, in clear agreement with the CT analysis performed at the TSs (see later).

The electrophilicity power of the simplest tetrazine **1** is 3.38 eV, a value that falls in the range of strong electrophiles within the ω scale.[26] Inclusion of the two electron-releasing thiomethyl groups on the TTZ **3** diminishes the electrophilicity of **1** to 3.10 eV. In spite of this fact, TTZ **3** remains as a strong electrophile. On the other hand, the inclusion of two electron-withdrawing carboxylic groups on the TTZ **1** increases the electrophilicity of the dicarboxymethyl derivative **2** to 3.64 eV. The asymmetrically disubtituted TTZs **5** and **6** present the largest electrophilicity values of this series, 3.72 and 3.70 eV, respectively.

The ER ethylenes **7**, **8**, and **9** have very low electrophilicity values, 0.17, 0.36, and 0.37 eV, respectively, being classified as marginal electrophiles. Recently, we have introduced an empirical (relative) nucleophilicity index, N, based on the HOMO energies.[23] The ER ethylenes **7**, **8**, and **9** have very large nucleophilicity values, 4.55, 3.56, and 3.17 eV, respectively, being classified as strong nucleophiles.[27] Therefore, the HDA reaction between the TTZ **5**, the strongest electrophile of this series, and ER vinylamine **7**, the strongest nucleophile, will take place along a polar process with very low activation energy. In this way, the corresponding HDA reaction takes place at room temperature in 1 min.[6] Note that the reaction of the TTZ **5** with the vinyl ethers **8** and **9** will have a lesser polar character, demanding larger reaction times, as can be seen in the original experimental reference: 2 h at the same reaction conditions (see Scheme 2).

Study of the Domino Reaction of the Asymmetric TTZ 5 with Vinylamine 7. The reaction between the asymmetric TTZ **5** and the vinylamine **7** to give the pyridazine **10** is a domino process that comprises three consecutive reactions (see Scheme 5): (i) a HDA reaction between **5** and **7** to give a bicyclic intermediate; (ii) a retro-Diels−Alder reaction with loss of nitrogen in this intermediate to give a 4,5-dihydropyridazine; and (iii) an elimination of pyrrolidine **18** to give the final pyridazine **10**. Due to the asymmetry of both reagents, TTZ **5** and the vinylamine **7**, two regioselective channels are feasible. In spite of the pyrrolidine elimination yielding a unique pyridazine **9**, the two regioisomeric channels were studied. An analysis of the stationary points found along the two regioisomeric channels indicates that both HDA and retro-Diels−Alder reactions take place along one-step mechanisms. Thus, six TSs, **TS11**, **TS12**, **TS21**, **TS22**, **TS31**, and **TS32**, two tricyclic intermediates, **IN11** and **IN12**, and two bicyclic intermediates, **IN21** and **IN22**, associated to the two regioisomeric approach modes of the pyrrolidine ring of **7** relative to the methylsulfinyl group present on the TTZ **5** were located and characterized.

The regioisomeric HDA reactions between TTZ **5** and the vinylamine **7** present very low activation barriers, 3.0 kcal/mol for **TS11** and 5.6 kcal/mol for **TS12**, as a consequence of the large polar character of these cycloadditions (see Table 2).[26] With the inclusion of diffuse functions at the B3LYP/6-31+G** level, the activation barriers rise slightly to 4.8 (**TS11**) and 7.8 (**TS12**) kcal/mol. These values are even lower than that obtained by Birney et al. for the HDA reaction of the symmetrically substituted TTZ **2** with the ER alkyne **15a**, 7.6 kcal/mol (see Scheme 3).[8] These HDA reactions are characterized by the nucleophilic attack of the most nucleophilic center of the vinylamine **7**, the C5 carbon atom, to the C1 or C4 carbon atoms of TTZ **5**. The energy difference between **TS11** and **TS12**, $\Delta\Delta E^{\#} = 2.6$ kcal/mol (3.0 kcal/mol at the B3LYP/6-31+G** level), is not large but sufficient for the unique formation of the cycloadduct **IN11** (see later). Therefore, the nucleophilic attack to the methylsulfinyl-substituted C1 carbon atom is favored over the attack to the methylthio-substituted C4 carbon atom. This behavior is in agreement with the experimentally observed nucleophilic displacement of the methylsulfinyl group of TTZ **5**.[6]

Formation of the tricyclic intermediates **IN11** and **IN12** is slightly endothermic in 0.9 and 2.1 kcal/mol, respectively. These intermediates, with a low barrier of 7.1 and 6.1 kcal/mol, respectively, lose nitrogen quickly to yield the bicyclic intermediates **IN21** and **IN22**, with the loss of nitrogen being very exothermic, ca. −50 kcal/mol. Therefore, this step of the domino reaction is irreversible.

The last step of these domino reactions is the elimination of a molecule of pyrrolidine **18** from the intermediates **IN21** and **IN22** to yield the final pyridazine **10**. Several mechanisms allow this elimination. First, we considered an intramolecular reaction in which the pyrrolidine moiety, acting as a base, eliminates the β hydrogen. An exploration of the potential energy surface for this reaction allowed us to find one TS associated to the β hydrogen abstraction by the basic pyrrolidine nitrogen. The activation barrier associated to the TS is very high: 44.3 (**TS31**) and 41.8 (**TS32**) kcal/mol, respectively. A part of this unfavorable energy can be related to the strain associated to the formation of a four-membered TS.[28] So, we considered an intermolecular elimination in which a second molecule of pyrrolidine **18** acts as a base removing the hydrogen atom (see Scheme 6). The intermolecular hydrogen abstraction from **IN21** via **TS41** had an activation barrier of 21.7 kcal/mol, being the process endothermic by 14.3 kcal/mol. That is, in the gas phase, the intermolecular process is 22.6 kcal/mol lower in energy than the intramolecular one.[28] With an unappreciable barrier, **IN41** eliminates pyrrolidine **18** to yield the final pyridazine **10**; this base-catalyzed elimination is exothermic by −14.7 kcal/mol.

As some species involved in these domino reactions have some polar character, and solvent effects can modify the relative energies, solvent effects of dichloromethane were considered by single-point energy calculations over the gas phase geometries.[29] The energy results are summarized in Table 2. With the inclusion of solvent effects, all structures are stabilized

(27) Jaramillo, P.; Domingo, L. R.; Chamorro, E.; Pérez, P. *J. Mol. Struct. (THEOCHEM)* **2008**, 68–72.

(28) Castillo, R.; Andrés, J.; Domingo, L. R. *Eur. J. Org. Chem.* **2005**, *470*, 5–4709.

(29) (a) Domingo, L. R. *J. Org. Chem.* **2001**, *66*, 3211–3214. (b) Arroyo, P.; Picher, M. T.; Domingo, L. R.; Terrier, F. *Tetrahedron* **2005**, *61*, 7359–7365.

SCHEME 5

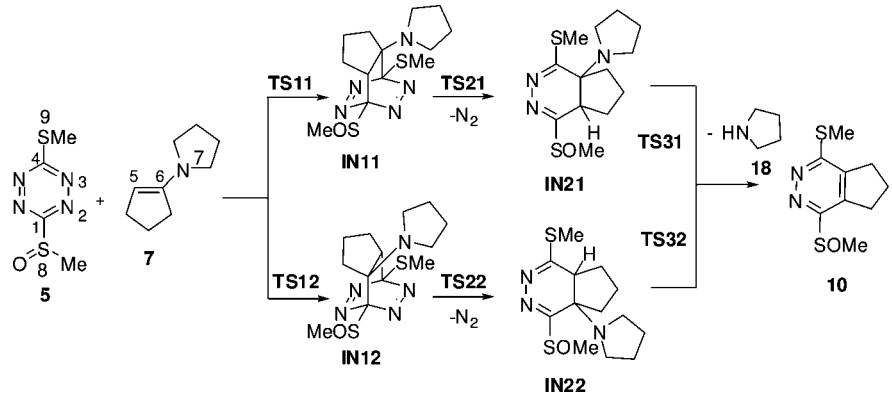

SCHEME 6

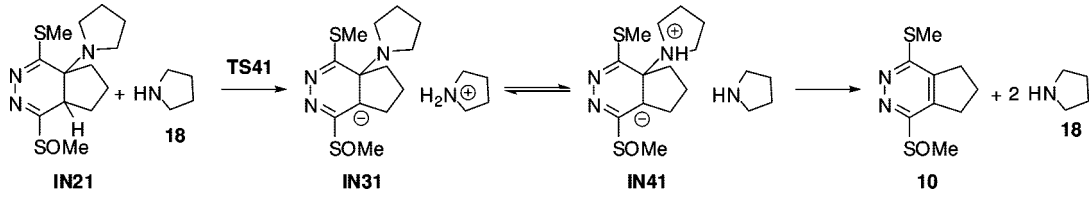

TABLE 2. BLYP/6-31G* Relative Energies (relative to 5 + 7, in kcal/mol) in the Gas Phase and in Dichloromethane of the Stationary Points Involved in the Domino Reaction between the Tetrazine 5 and the Vinylamine 7

	gas phase	dichloromethane
TS11	3.0	4.2
IN11	0.9	3.5
TS21	8.0	11.1
IN21	−49.4	−46.7
TS31	−5.1	−6.0
TS12	5.6	7.5
IN12	2.1	5.0
TS22	8.2	11.9
IN22	−49.3	−46.0
TS32	−7.5	−7.1
10 + 18	−56.0	−54.7
TS41	21.7	18.1
IN31	14.3	8.1

between 7 and 12 kcal/mol. **TS11** and **TS12** are stabilized by 9.1 and 8.4 kcal/mol. However, the reagents are more stabilized, 10.3 kcal/mol, as a consequence of the large polar character of TTZ **5**. So, the activation barrier of these HDA reactions increases slightly. In addition, in dichloromethane, **TS11** is slightly more stabilized than **TS12**. Consequently, the regioselectivity increases to 3.3 kcal/mol, in clear agreement with the experimental outcome. Finally, in dichloromethane, the activation barrier of the intermolecular elimination reaction via **TS41** decreases to 18.1 kcal/mol.

Both gas phase and solvent effect calculations estimate that the formation of the intermediates **IN11** and **IN12** is slightly endothermic. In addition, **TS21** and **TS22** are located above **TS11** and **TS12** in energy (see Table 2). This means that the step associated to the loss of nitrogen would be the rate-determining one of these domino processes, in disagreement with the regioselectivity experimentally observed. In dichloromethane, **TS21** is only 0.8 kcal/mol lower in energy than **TS22**. Recent studies have shown that B3LYP calculations fail to compute the enthalpy energies of the formation of C−C bonds in bicyclic and related compounds. To test the B3LYP energies,

TABLE 3. MP3/6-31G*//B3LYP/6-31G* Relative Energies (in kcal/mol) of the Stationary Points Involved in the Two First Steps of the Domino Reaction between the Tetrazine 5 and the Vinylamine 7

TS11	−0.9	**TS12**	0.7
IN11	−21.6	**IN12**	−19.2
TS21	−9.2	**TS22**	−8.4
IN21	−75.3	**IN22**	−75.3

MP3/6-31G* single-point energy calculations were performed.[30] The energy results are summarized in Table 3. The MP3 activation barriers associated to these polar HDA reactions are slightly lower than those obtained at the B3LYP level. However, it is worth noting that there is a strong disagreement about the relative energies of the intermediates **IN11** and **IN12**. At the MP3 level, formation of these intermediates is strongly exothermic: −21.6 and −19.2 kcal/mol, respectively. These results point out the poor accuracy of the B3LYP calculations to describe the thermochemistry of these HDA reactions. The MP3 barriers of the nitrogen loss, 12.4 and 10.8 kcal/mol, are slightly larger than those obtained at the B3LYP level. Now, at the MP3 level, **TS21** and **TS22** are 8.4 and 9.1 kcal/mol below **TS11** and **TS12**, respectively. This means that the HDA reaction is the rate-determining step of the domino reaction, and as a consequence, this step is responsible for the regioselectivity experimentally observed.

Because the three steps of the domino reaction between TTZ **5** and the vinylamine **7** involve chemical processes of different molecularity, the total and relative free energies associated to the stationary points of this domino reaction were computed at the reaction conditions (25 °C and in dichloromethane). The energy data are collected in the Table 4 while a schematic representation of the free energy profile for the domino reaction is drawn in Figure 1. The B3LYP/6-31G* free energy of **IN11** has been corrected by a factor of −22.5 kcal/mol obtained from the MP3 calculations. After **IN11**, all relative energies are referenced to this intermediate.

(30) Polo, V.; Domingo, L. R.; Andres, J. *J. Org. Chem.* **2006**, *71*, 754–762.

TABLE 4. B3LYP/6-31G* Relative Free Energies (ΔG and ΔG_{cor}, in kcal/mol; calculated at 25 °C, 1 atm in dichloromethane) of the More Relevant Stationary Points Involved in the Domino Reaction between the TTZ 5 and the Vinylamine 7

	ΔG	ΔG_{cor}
TS11	20.7	20.7
IN11	22.8	0.3[a]
TS21	31.1	8.6[a]
IN21	−41.0	−63.5[a]
TS41	19.8	−43.8[a]
IN31	13.5	−50.0[a]
TS12	24.9	24.9
IN12	25.3	2.8[a]
10	−74.3	−96.8[a]

[a] Corrected by a factor of −22.5 kcal/mol (see text).

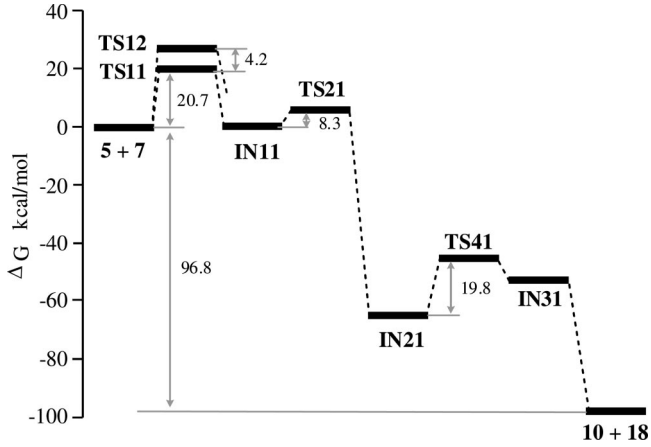

FIGURE 1. Free energy profile for the most favorable reaction path of the domino reaction between TTZ **5** and the vinylamine **7** in dichloromethane. The **TS12** of the rate-determining step of the lesser favorable reaction path has been included for comparative purposes. The relative free energy of **IN11** has been scaled from the MP3/6-31G* calculations (see text).

With the inclusion of the thermal corrections and the entropies to the electronic energies, the free activation energy associated to the HDA reaction via **TS11** rises to 20.7 kcal/mol. The unfavorable activation entropy associated to the bimolecular HDA reaction between **5** and **7**, −52 cal/(mol·K), is responsible for this value. The relative free energy between **TS11** and **TS12** rises to 4.2 kcal/mol, a value in clear agreement with the total regioselectivity experimentally observed.[6] The intermediate **IN11**, with a low free activation energy, 8.3 kcal/mol, quickly loses nitrogen to yield **IN12**, with the reaction being strongly exergonic by −64 kcal/mol. From this intermediate, the free activation energy associated to the bimolecular β-elimination, 19.8 kcal/mol, is slightly lower than that for the HDA reaction. The overall domino reaction is strongly exergonic by −96.8 kcal/mol. These energy results indicate that after the HDA reaction between **5** and **7**, the two subsequent elimination reactions take place spontaneously and irreversibly toward the final pyridazine **10** (see Figure 1).

The geometries of the TSs involved in the HDA reactions of the TTZ **5** with the vinylamine **7** and the subsequent loss of nitrogen are given in Figure 2. At the TSs associated to the polar HDA reactions between **5** and **7**, the length of the C−C forming bonds are 2.067 Å (C1−C5) at **TS11** and 2.114 Å (C4−C5) at **TS12**, whereas the distances between the two carbons that do not participate at this stage of the cycloaddition (see later) are 3.197 Å (C4−C6) at **TS11** and 3.061 Å (C1−C6) at **TS12**. With the inclusion of diffuse functions at the B3LYP/6-31+G** level, the **TS11** is slightly delayed while the geometry of **TS12** is not modified. The extent of the asynchronicity of the bond formation in a cycloaddition reaction can be measured through the difference between the lengths of the two σ bonds that are being formed in the reaction, i.e., Δr = dist1 − dist2. The large values found for Δr at the TSs, 1.13 at **TS11** and 0.94 at **TS12**, indicate that they correspond to highly asynchronous bond-formation processes. At these TSs, the length of the C6−N7 bond is slightly diminished as a consequence of the participation of the N7 nitrogen lone pair at the nucleophilic attack.

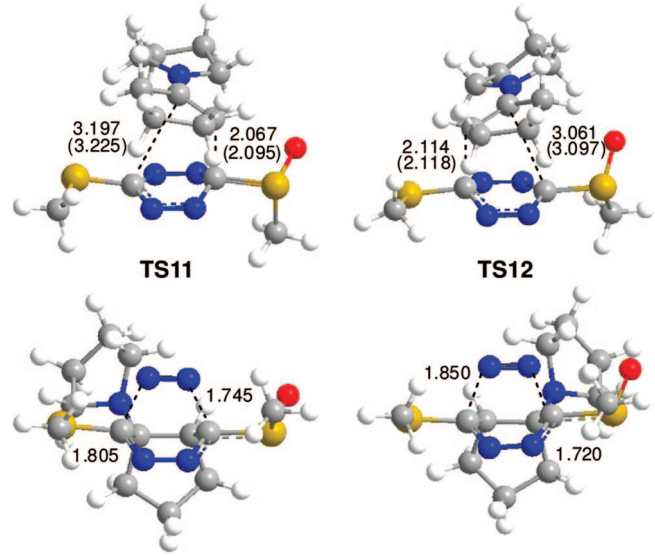

FIGURE 2. B3LYP/6-31G* transition state geometries involved in the two regiosiomeric paths of the HDA reaction and nitrogen extrusion of the domino reaction of TTZ **5** with the ER vinylamine **7**. The B3LYP/6-31+G** parameters are given in parentheses. The distances are given in Å.

An analysis of the IRC from these highly asynchronous TSs to the corresponding [4+2] cycloadducts indicates that these polar HDA reactions have *two-stage* mechanisms.[31] At the first stage of the reaction, only the C1−C5 at **TS11** and the C4−C5 at **TS12** bonds are being formed along the nucleophilic attack of the terminal C5 carbon of the vinylamine **7** to the C1 and C4 electrophilic positions of the TTZ **5**, opening the two regiosiomeric pathways. Along these nucleophilic attacks, the N7 nitrogen lone pair is being delocated over the positively charged ethylenic C6 carbon of the vinylamine **7**. This behavior, which rules out the participation of the C6 carbon on the formation of the second C−C bond at this stage of the reaction, is responsible for the nonconcerted character of these *two-stage* reactions.

At the TSs associated to the loss of nitrogen, the lengths of the C−N breaking bonds indicate that these TSs correspond to synchronous concerted processes (see Figure 2). These lengths indicate that these TSs have a much earlier character in clear agreement with the low barriers and the strong exothermic character of these reactions.[31] A small asynchronicity is found, Δr = 0.06 at **TS21** and 0.13 at **TS22**, as a consequence of the asymmetry of TTZ **5**.

(31) Domingo, L. R.; Saéz, J. A.; Zaragozá, R. J.; Arnó, M. *J. Org. Chem.* **2008**, *73*, 8791–8799.
(32) Hammond, G. S. *J. Am. Chem. Soc.* **1955**, *77*, 334–338.

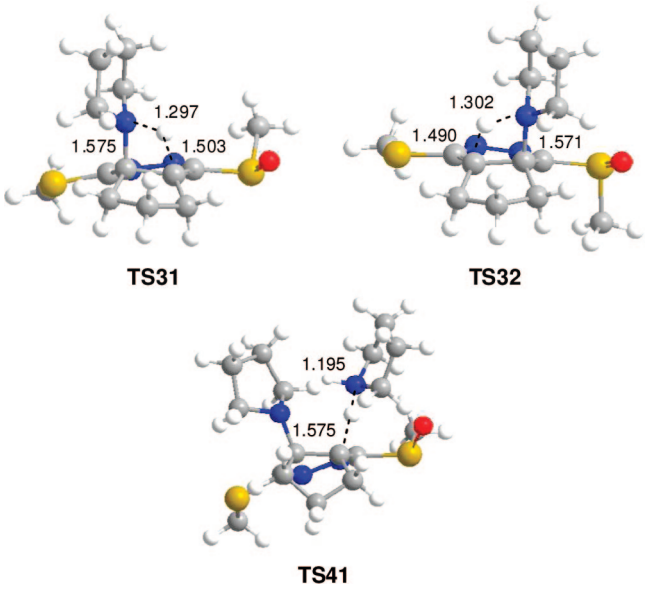

FIGURE 3. B3LYP/6-31G* transition state geometries involved in the intramolecular, **TS31** and **TS32**, and the intermolecular, **TS41**, hydrogen elimination reactions. The distances are given in Å.

The geometries of the TSs involved in the hydrogen elimination reactions are given in Figure 3. The lengths of the C−H breaking and H−N forming bonds at these TSs are 1.503 and 1.297 Å at **TS31**, 1.490 and 1.302 Å at **TS32**, and 1.575 and 1.195 Å at **TS41**. These lengths point out asynchronous processes in which the proton transfer process is very advanced. The more favorable intermolecular **TS41** is slightly more advanced.

The electronic structure of the TSs involved in the HDA reaction was analyzed by using the Wiberg bond order[33] (BO) and the natural charges obtained by a NBO analysis. The BO values of the C−C forming bonds at the TSs are 0.45 (C1−C5) at **TS11** and 0.44 (C4−C5) at **TS12**, whereas these values between the two carbons that do not participate at this stage of the reaction are 0.04 in both TSs. The more favorable **TS11** is slightly more advanced. The BO values of the C6−N7 bond in both regioisomeric paths, 1.34 and 1.37, point out a large π character of this bond as a consequence of the participation of the N7 nitrogen lone pair in these polar reactions. These BO values indicate that these TSs are associated to a two-center addition, characteristic of a polar process, and are far from a concerted pericyclic one.

The natural population analysis (NPA) allows the evaluation of the CT at these polar HDA reactions. The B3LYP/6-31G* natural atomic charges at the TSs associated to the two-center interactions were shared between the TTZ **5**, which acts as a very good electrophile, and the ER vinylamine **7**, which acts as a very good nucleophile. The net charge at the TTZ fragment at these TSs is predicted to be 0.43 e at **TS11** and 0.46 e at **TS12**. These large values, which are in agreement with the dipolar moment of the TSs, 4.41 and 3.88 debye, respectively, point out the large zwitterionic character of the TSs, and the large polar character of these HDA reactions. Note that the dipolar moment at the intermediates **IN11** and **IN12** decreases to 2.61 and 3.31, respectively. The larger dipole moment of **TS11** than **TS12** is in agreement with the larger solvation of the former, and with the increase of the regioselectivity in dichloromethane.

(33) Wiberg, K. B. *Tetrahedron* **1968**, *24*, 1083–1096.

Study of the Regioselectivity in the HDA Reaction of the Asymmetric TTZ 5 with the Vinyl Ethers 8 and 9. Since the HDA reaction of these domino processes is the rate- and regioselective-determining step of these reactions, the two regioisomeric channels associated to the HDA reactions of the asymmetric TTZ **5** with the vinyl ethers **8** and **9** were also studied in order to explain the regioselectivity experimentally observed (see Scheme 7). The energetic results are given in Table 5.

The free activation energies associated to the TSs are 30.5 (**TS13**), 34.5 (**TS14**), 29.1 (**TS15**), and 32.5 (**TS16**) kcal/mol. Some conclusions can be redrawn from these values: (i) the free activation energies associated to the more favorable reactive channels are ca. 10 kcal/mol higher than that for the reaction between the TZZ **5** and the vinylamine **7**, in clear agreement with the larger reaction time required by the formers (see Scheme 2). These energetic results are also in agreement with the lesser nucleophilic character of the vinyl ethers **8** and **9** than the vinylamine **7**; (ii) the regioselectivity measured as $\Delta\Delta G^{\#}$ between the two regioisomeric TSs, 4.1 (**8**) and 3.4 (**9**) kcal/mol, are of the same order as that computed for the HDA reaction with **7**, 4.2 kcal/mol; (iii) interestingly, the $\Delta\Delta G^{\#}$ for the HDA reaction with the dihydrofurane **9** is lower than those for the reactions with the ethylene derivatives **7** and **8**, and these energies are in clear agreement with the experimental results, and while the reaction with **8** gives a unique regiosiomer **12**, respectively, the reaction with **9** also yields 5−10% of the regioisomeric cycloadduct **20**; and (iv) the B3LYP/6-31G* calculations consider these DA reactions as endergonic processes by 17.1 and 9.0 kcal/mol. As for the reaction with **7**, the DFT calculations underestimate the reaction energies associated to these HDA reactions.

The geometries of the TSs are given in Figure 4. The lengths of the two C−C forming bonds at these TSs indicate that they also correspond to high asynchronous bond formation processes. At these TSs, the shorter distance also corresponds to the C−C bond formation involving the C5 carbon atom of the vinyl ether **8** and **9**, that is, the most nucleophilic center of these ER ethylenes. The asynchronicity at the TSs, $\Delta r = 0.91$ at **TS13**, 0.78 at **TS14**, 0.60 at **TS15**, and 0.39 at **TS16**, indicate that these TSs are less asynchronous than those associated to the HDA reaction of the vinylamine **7**.

The BO values of the C−C forming bonds at the TSs are 0.58 (C1−C5) and 0.11 (C4−C6) at **TS13**, 0.52 (C4−C5) and 0.12 (C1−C6) at **TS14**, 0.50 (C1−C5) and 0.16 (C4−C6) at **TS15**, and 0.43 (C4−C5) and 0.18 (C1−C6) at **TS16**.

The CT at these regioisomeric TSs, 0.36 e at **TS13**, 0.38 e at **TS14**, 0.32 e at **TS15**, and 0.33 e at **TS16**, indicates that these HDA reactions also have a large polar character. Note that these values are lower than that for the HDA reaction with the vinylamine **7**, in clear agreement with the lesser nucleophilic character of the vinyl ethers **8** and **9** and with the larger free activation energy of the reaction with the vinyl ethers. Note also that the CT is slightly larger at the more energetic regioisomeric TSs.

Which Is the Origin of the Unexpected Regioselectivity of the HDA Reactions of the Asymmetric Substituted TTZs 5 and 6? A simple observation of the TSs involved in the regioselective HDA reactions (see Figures 2 and 4) discards any steric effect as responsible for the regioselectivity. Two geometrical behaviors exclude these unfavorable interactions: (i) at these highly asynchronous TSs, the most advanced C−C

SCHEME 7

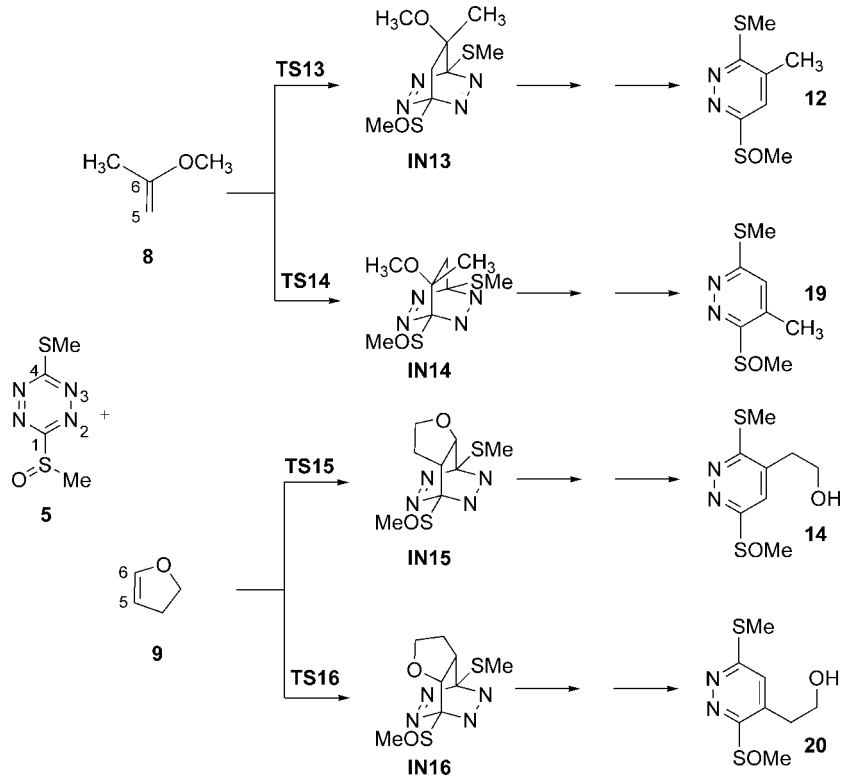

TABLE 5. B3LYP/6-31G* Relative Energies (Δ*E*, kcal/mol) and Free Energies (Δ*G*, kcal/mol; calculated at 25 °C, 1 atm in dichloromethane) of the Stationary Points Involved in the HDA Reaction between the TTZ 5 and the Vinyl Ethers 8 and 9

	Δ*E*	Δ*G*
TS13	15.2	30.4
TS14	19.7	34.5
IN13	−2.6	17.1
IN14	−4.1	16.5
TS15	12.1	29.1
TS16	15.4	32.5
IN15	−12.0	9.0
IN16	−12.8	7.9

bond formation involves the small methylene group of the ER ethylenes, which corresponds to the most nucleophilic center of these reagents, and (ii) the free rotation of the two sulfur substituents at the TTZs allows an *anti* rearrangement of the methyl groups, dismissing any steric interaction.

As has been indicated, the regioselectivity, measured as the energy difference between the regioisomeric TSs, $\Delta\Delta E^{\#}$, ranges from 2.6 to 4.6 kcal/mol and is not large compared with other regioselective polar Diels–Alder reactions in which $\Delta\Delta E^{\#}$ ranges between 4.2 and 25.9 kcal/mol, a value that increases with the polar character of the DA reactions.[34] On the other hand, the lengths of the C1–S8 and C4–S9 bonds at the regiosiomeric TSs, 1.87 and 1.77 Å at **TS11** and 1.82 and 1.81 Å at **TS12**, are closer to those at the TTZ **5** of 1.85 and 1.76 Å, respectively, indicating that, at these TSs, there is not a large π conjugation toward the two sulfur substituents.

A NPA of the asymmetric TTZ **5** indicates that the TTZ core exerts a strong EW effect relative to the two sulfur substituents. Thus, the charge at the TTZ core is −0.57 e, whereas at the methylsulfinyl and thiomethyl groups it is +0.25 and +0.32 e, respectively (see Scheme 8). This behavior points to the large electronegative character of the TTZ core relative to the two sulfur substituents. This analysis made at two regioisomeric TSs reveals that a large amount of the charge transferred from the ER ethylenes to the TTZ along the cycloaddition remains at the TTZ core: −0.29 e at **TS11** and −0.27 e at **TS12**, respectively. Therefore, in spite of the CT being slightly larger at the more energetic TSs, the charge on the TTZ core is slightly larger at the lesser energetic TSs (see Scheme 8). This behavior can be explained by the fact that at the more energetic regioisomeric TSs, the nucleophilic attack of the ER ethylene takes place at the conjugated *para* C4 position relative to the methylsulfinyl group, favoring a slight charge delocation toward this group and, in consequence, decreasing the charge at the

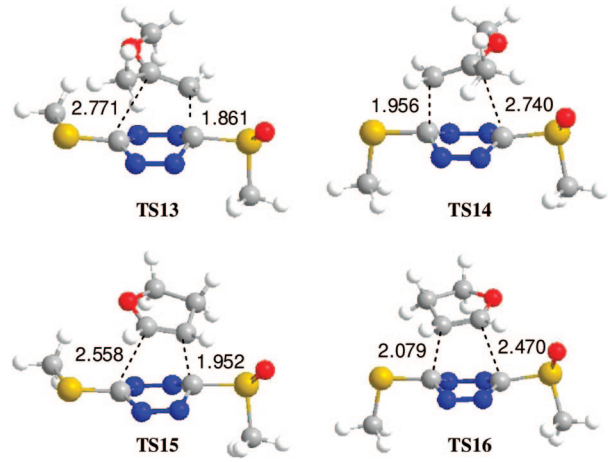

FIGURE 4. B3LYP/6-31G* transition state geometries involved in the two regioisomeric paths of the HDA reactions of TTZ **5** and the ER vinyl ethers **8** and **9**. The distances are given in Å.

(34) Domingo, L. R.; Arno, M.; Andres, J. *J. Org. Chem.* **1999**, *64*, 5867–5875.

SCHEME 8. NPA at the TTZ 5 and TSs Associated with the HDA Reaction of 5 with 7

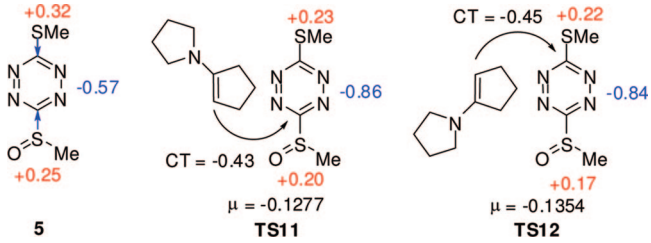

electronegative TTZ core. This behavior makes this nucleophilic attack mode energetically lesser favorable than the attack at the C1 position.

From the point of view of the conceptual DFT, this phenomenon could be explained by taking the mean electronic chemical potential of both TTZ **5** and vinylamine **7** reagents, $\mu_{\mathbf{R}} = -0.1177$ au, and comparing it with that obtained for **TS11** ($\mu = -0.1277$ au) and **TS12** ($\mu = -0.1354$ au) (Figure 5). The most favored reaction path is that where the $\Delta\mu_{\mathbf{R}\rightarrow\mathbf{TS}}$ is the lowest, as it is related to the energy needed by the system to reorganize the charge along the reaction.[35] The larger $\Delta\mu$ obtained for **TS12**, $\Delta\mu_{\mathbf{R}\rightarrow\mathbf{TS12}} = 0.0177$ au, than that obtained for **TS11**, $\Delta\mu_{\mathbf{R}\rightarrow\mathbf{TS11}} = 0.0100$ au, indicates that the reaction path via **TS11** will be energetically more favorable, in clear agreement with the energy results. This behavior, which is also observed at the reactions with the vinyl ether **8** and **9** (see Figure 5), accounts for the unexpected regioselectivity experimentally observed at these HDA reactions. Interestingly, the $\Delta\Delta\mu$ of the three pairs of regioisomeric TSs, in the range of 4.8 to 5.8 kcal/mol, is closer to the $\Delta\Delta E^{\#}$ of these HDA reactions, between 2.6 and 4.5 kcal/mol.

Although in the gas phase the energy difference caused by this phenomenon at the two regioisomeric TSs is not large, it is sufficient to make these HDA reactions regioselective. This behavior, which cannot be explained by a FMO analysis of the MO coefficients as was indicated by Boger,[6] allows us to explain the unexpected regioselectivity of these asymmetric TTZs.

Finally, it is worth noting that the electronic chemical potential and the electrophilicity of the carbamate derivative **6** are similar to those at the thiomethyl derivative **5** (see Table 1). Therefore, the (benzyloxycarbonyl)amino group present in the TTZ **6** is expected to exert a similar electronic effect as the thiomethyl group present in the TTZ **5** in these regioselective HDA reactions.

Conclusions

The regioselective HDA reactions of asymmetric 1,4-disubstituted TTZs with ER ethylenes has been studied with DFT methods at the B3LYP/6-31G* level of theory. These reactions are domino processes that comprise three consecutive reactions: (i) a polar HDA reaction between the TTZ and the ER ethylene; (ii) a retro-Diels−Alder reaction with loss of nitrogen; and (iii) a β-hydrogen elimination with formation of the final substituted pyridazines. The first polar HDA reaction, which is associated to the nucleophilic attack of the ER ethylene to the electrophilically activated TTZ, is the rate-determining step of the domino process. The large electrophilic character of the TTZs, together with the large nucleophilic character of the ER ethylenes are responsible for the large polar character of the

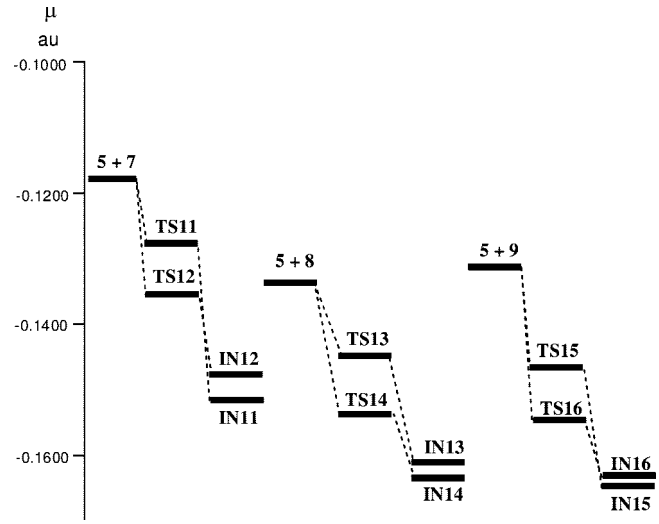

FIGURE 5. Changes in electronic chemical potential μ along the two regioisomeric channels.

HDA reactions and the low activation energies found. The formed bicyclic intermediate irreversibly loses nitrogen with a very low barrier. Finally, an intermolecular β-elimination affords the final substituted pyridazine. The more favorable attack of the most nucleophilic center of the ER ethylene to the C1 carbon of the TTZ containing the methylsulfinyl substituent over the attack to the C4 carbon atom containing the methylthio one is responsible for the regioselectivity experimentally observed. This behavior is supported by a further study of the regioselectivity on the HDA reaction between the asymmetric TTZ and two asymmetric vinyl ethers, which were shown experimentally to be regioselective.

Thermodynamic calculations performed at the reaction conditions indicate that after the HDA reaction between the TTZ and the ER ethylene, the two subsequent elimination reactions take place spontaneously and irreversibly toward the final pyridazine. Therefore, the HDA reaction is the regioselective step of these domino processes. The relative free energies in dichloromethane of the two regioisomeric TSs involved in the studied polar HDA reactions, $\Delta\Delta G^{\#}$, which range from 3.4 to 4.2 kcal/mol, are in reasonable agreement with the regioselectivity experimentally observed.

The unexpected regioselectivity of these HDA reactions, which was not explained with the FMO theory, is well stated, using the polar cycloaddition model and the reactivity indexes defined within the conceptual DFT. Although the nucleophilic attack of the ER ethylene over the *para* position relative to the methylsulfinyl substituent could favor the charge transfer at these polar HDA reactions, this attack is energetically more unfavorable because it diminishes the electron density at the electronegative TTZ core. This behavior is manifested by the minor changes on the electronic chemical potential found along the more favorable regioisomeric TSs.

Acknowledgment. This work was supported by research funds provided by the Ministerio de Ciencia e Innovación of the Spanish Government (project CTQ2006-14297/BQU).

Supporting Information Available: Complete citation for ref 18; B3LYP/6-31G* total energies in the gas phase and in dichloromethane and the total enthalpies, entropies, and free energies in dichloromethane of the stationary points involved

(35) Ayers, P. W.; Parr, R. G. *J. Am. Chem. Soc.* **2000**, *122*, 2010–2018.

in the domino reaction between the tetrazine **5** and the vinylamine **7**; MP3/6-31G*//B3LYP/6-31G* total energies of the stationary points involved in the two first steps of the domino reaction between the tetrazine **5** and the vinylamine **7**; B3LYP/6-31G* total energies and total enthalpies, entropies, and free energies in dichloromethane of the stationary points involved in the HDA reaction between the TTZ **5** and the vinyl ethers **8** and **9**; B3LYP/6-31G* Cartesian coordinates of the TSs and intermediates; and B3LYP/6-31+G** Cartesian coordinates of the regioisomeric **TS11** and **TS12**. This material is available free of charge via the Internet at http://pubs.acs.org.

JO802822U